

# 3D point cloud segmentation using GIS

Chao-Jung Liu, Vladimir Krylov & Rozenn Dahyot

*ADAPT Centre, School of Computer Science and Statistics, Trinity College Dublin, Ireland*

## Abstract

In this paper we propose an approach to perform semantic segmentation of 3D point cloud data by importing the geographic information from a 2D GIS layer (OpenStreetMap). The proposed automatic procedure identifies meaningful units such as buildings and adjusts their locations to achieve best fit between the GIS polygonal perimeters and the point cloud. Our processing pipeline is presented and illustrated by segmenting point cloud data of Trinity College Dublin (Ireland) campus constructed from optical imagery collected by a drone.

**Keywords:** Segmentation, semantic labelling, 3D point clouds, 3D environment.

## 1 Introduction

Up-to-date accurate 2D and 3D maps are growing increasingly important for localisation and navigation employed by both humans and machines. Various technologies and data collection modalities are available nowadays to capture and encode a digital twin of the world such as Lidar [Laefer et al., 2017] and drone imagery [Byrne et al., 2017]. Once created, such digital twins can be seamlessly manipulated and visualised with the help of game engines, and used in applications, such as education (e.g., driving simulators), and entertainment (e.g., virtual visits and gaming [Haahr, 2017]). More recently these virtual environments have also found applications in providing valuable labeled data for training machines using data driven artificial intelligence. For instance project Airsim<sup>1</sup> uses the Unreal game engine to provide training data for autonomous drones and cars.

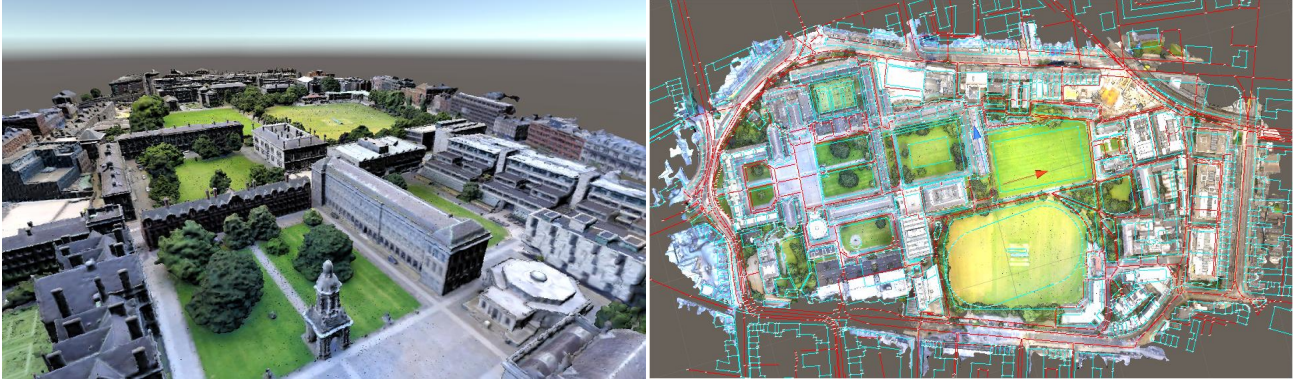
In this paper, our aim is to label automatically unstructured geolocated 3D point cloud data. For this purpose we propose to register heterogeneous sources of information: the semantic information provided by OpenStreetMap (OSM) and 3D point clouds covering the same geographic area (Fig. 1). We show that the registration of these two sources of information allows one to segment the point cloud in useful semantic units with arbitrary geometrical shapes. After introducing some related work (Sec. 2), our approach is presented in Section 3.

## 2 Related Work

Structure from motion techniques have been widely used for reconstruction of large scale scenes and image geo-location. Practically, it has become a cheaper alternative to costly high-end LiDAR technology. Structure from motion relies on keypoint detection, image matching, bundle adjustment and, finally, generation of dense point clouds. These points can then be condensed into meshes and be presented in game engine as terrain (cf. Fig. 1a). For instance, Agarwal et al. [Agarwal et al., 2009] use a large collection of pictures harvested from the web to create a sparse point cloud of a city. Bódis-Szomorú et al. [Bódis-Szomorú et al., 2016] proposed to reconstruct a mesh of a city area by registering and fusing two point clouds, one airborne and the other generated from street view and aerial images to reconstruct the city view, and then generate

---

<sup>1</sup><https://github.com/Microsoft/AirSim>



(a) Trinity 3D model dataset [Byrne et al., 2017]

(b) Overlay OSM data onto game terrain

**Figure 1:** 3D point cloud of Trinity College Dublin campus, 2015.

the mesh by using fusion techniques. Rumpler et al. [Rumpler et al., 2012] register OSM data for retrieving the information of outlines of buildings in the form of 2D vectors, and use them with satellite pictures to generate 3D mesh building. Bulbul and Dahyot [Bulbul and Dahyot, 2017] reconstruct cubical model of a city using OSM geolocated building footprints and heights, and associate textures extracted from Google Street view imagery to recover building facade. The resulting 3D city model is then used in a game engine for visualisation of social media activity in the area, using pictures posted on social media platforms.

There is a large body of work for image region labeling into generic categories such as cars, trees or buildings. For instance, Tighe and Lazebnik [Tighe and Lazebnik, 2010] proposed an image parsing method to segment the region of images by trained descriptors. The semantic labels are classified by predefined class for geometric / semantic context. The semantic labeling work is conducted through all of the overlapping images for reconstruction, which is very time consuming. Having a 3D mesh generated multiple view imagery, Riemenschneider et al. [Riemenschneider et al., 2014] improve computation complexity and accuracy by predicting the best image view for clustering and propagate the labels to the mesh. It is shown to be more efficient than clustering of all images and merging labels for a same object in the scene. Tchapmi et al. [Tchapmi et al., 2017] label raw point clouds using neural networks with Conditional Random Field to predict class of each point in the cloud. Kaiser et al. [Kaiser et al., 2017] segment the 2D aerial imagery into object by using the data from OSM, transforming geographic coordinate to local pixel coordinates, and use neural network architecture to refine the boundary to make a finer-grained labeling for objects. Becker et al. [Becker et al., 2017] proposed to classify photogrammetric 3D point clouds into specific classes (e.g. road, building, vegetation).

Krylov et al. [Krylov et al., 2018] proposed to geolocate street furniture from Google Street View (GSV) imagery using fully convolutional neural networks for object segmentation and distance estimation followed by a Markov Random Field to coherently geolocate individual objects in images. This was extended in [Krylov and Dahyot, 2018] to the fusion of street level imagery and LiDAR data to object detection at increased spatial accuracy. Similarly, Branson et al. [Branson et al., 2018] use GSV images together with optical satellite imagery for cataloguing street trees.

### 3 Geolocated Data Registration

Our approach is demonstrated using the data for Trinity College Dublin Campus recorded using a drone in 2017, which is available open source [Byrne et al., 2017]. Our methodology employs the 3D point cloud generated from drone imagery (Sec. 3.1) but can also be applied to Lidar data (e.g [Laefer et al., 2017]). We employ OSM data as GIS source of information [Rumpler et al., 2012, Kaiser et al., 2017, Bulbul and Dahyot, 2017].

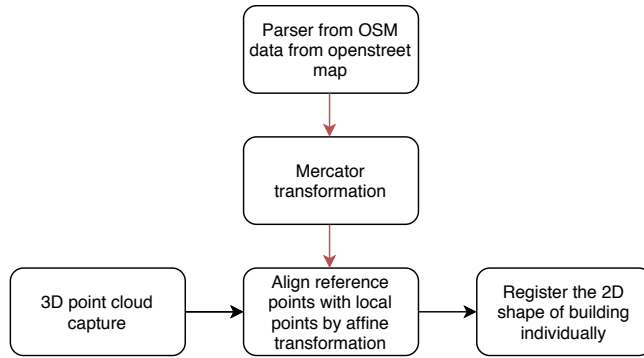


**Figure 2:** Registration is performed in two steps: affine registration for the whole dataset, followed by a separate position adjustment for each building.

### 3.1 3D point clouds generated from drone imagery

The Trinity campus mesh has been generated from optical imagery captured by a drone [Byrne et al., 2017] in 2017. Pix4D software<sup>2</sup> has been employed to process the images to generate the geolocated point cloud using structure from motion techniques.

### 3.2 OSM data structure and parsing

To acquire geolocation and semantic label data, we employ the OSM API that allows one to extract information about specific geographic area from their database in XML format. We use this interface to collect semantic information about the Trinity campus. The XML dump file contains all 3 types of OSM attributes: ways, nodes and relations. Ways are used to encode polygon-shaped areas like buildings, roads, etc. A way contains semantic labels (tags) and references to corresponding nodes. Each node contains the geolocation (longitude and latitude) of an individual point on the map (e.g., corner of a building). Relations are used to model local logical or geographic relationships between objects. Using the name of any individual building we can search among all the way attributes to find all the nodes establishing its location inside the Trinity campus.

### 3.3 Mercator projection

OSM uses WGS84 spatial reference system. This is the reference system also used by GPS. The corresponding coordinates are referred to as longitude and latitude. WGS84 models Earth as a spheroid. The real shape is however ellipsoidal, i.e. flat at both poles. To resolve this inconsistency, the Mercator projection<sup>3</sup> is employed.

### 3.4 User defined correspondences between heterogeneous data streams

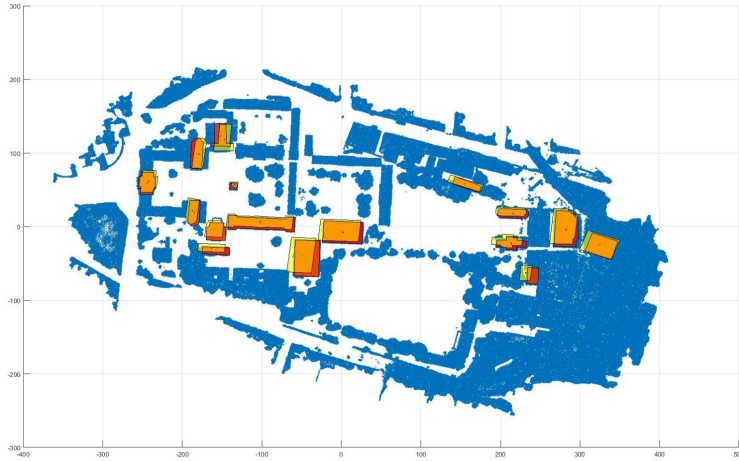
To align the reference location from Mercator projection to 3D model, we manually selected 18 correspondences (control points) between the two media streams to estimate an affine transformation matrix handling translation, rotation and scale with Least Squares.

The center of Trinity campus model (0,0) is on the Museum building, has OSM coordinate (53.34380,-6.25532) and Mercator projection coordinate(-696339.0371489801,7012543.77625507).

Fig. 2 presents our processing pipeline.

<sup>2</sup><https://pix4d.com/>

<sup>3</sup><https://wiki.openstreetmap.org/wiki/Mercator>



(a) Intersection (orange) between OSM building positions (yellow) and 3d point cloud ground truth locations (red).

	IoU	Distance (meters)
Average	0.567	5.594
Median	0.607	4.871

(b) Distance between centroids defined by OSM and 3d point cloud across 16 buildings.

**Figure 3:** Fit between point cloud data and OSM GIS data after global registration.

### 3.5 Evaluation of Global Affine registration with user defined correspondences

To evaluate how accurate the geo-locations of nodes from OSM fit the considered point cloud dataset, we report assessment on 16 buildings across the campus. We also manually label the point cloud by photo-interpretation to have a ground truth of semantic units corresponding to these 16 buildings. Each building is defined by its perimeter, i.e. a polygon shape on x-y plane in orthographic view (see red polygons in Fig. 3a). The information about building locations coming from OSM is reported as yellow polygons in Fig. 3a. We compare these two polygons as 2D shapes (discarding the third dimension of data) to assess the correspondance via overlap using *Intersection of Unions* (IoU) [Csurka et al., 2013]. The IoU is a real number between 0 to 1, where higher values mean better fit (equivalently, stronger overlap). We compute the shape's centroid points and use these to find distance between polygons.

As can be seen (Fig. 3a), there is a substantial misalignment between geolocations reported by OSM and 3d point cloud. This is mainly because one single affine transformation does not capture well the deformation between the two streams of information. Furthermore, the location information in OSM is crowd-sourced and is not always of the highest spatial accuracy. Figure 3b reports the averages and median values for IoU and the distance between OSM and 3d point cloud polygons' centroids. Fig. 4 demonstrates the IoU for each of building and it reflects to the misalignment for each of building.

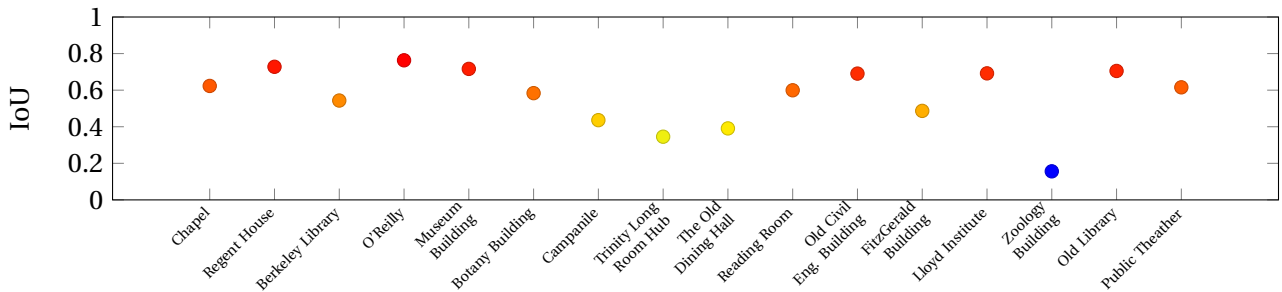


**Figure 4:** IoU per building after global affine registration.

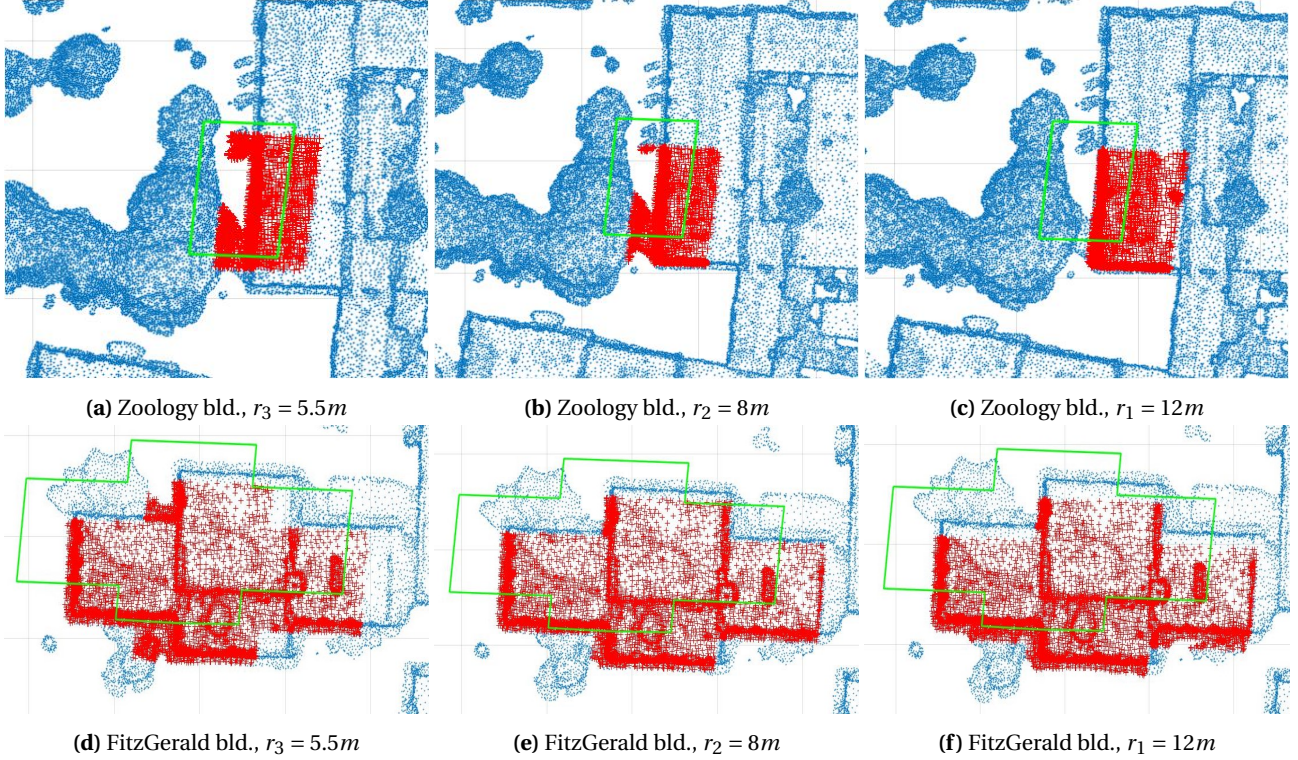


**Figure 5:** 2D point cloud after ground removal (blue points) and the segmentation (red points) obtained by the proposed OSM adjustment procedure for various search radii  $r$  exemplified on Zoology and FitzGerald buildings. Green polygons represent the original OSM building positions.

## 4 Adjustment of OSM locations

Alongside the considered 16 buildings our 3d point cloud is comprised of other points, describing ground, trees and other buildings. We first remove the ground points by elevation surface thresholding using CloudCompare (available at <https://www.danielgm.net/cc/>). We then discard the third coordinate data in the 3d point cloud (elevation above the reference level) transforming it into 2d point cloud  $D_{2d}$ .

We employ IoU as the main metric to assess the quality of fit between the data and ground truth locations. In order to improve IoU for buildings, we propose to estimate the optimal translation from OSM-defined positions towards 3d point cloud clusters. We assume that the spatial orientation (rotation) and scaling are correct in OSM. In other words, to identify parts of the point cloud that correspond to specific buildings we assume that the polygon defining the perimeter of the building is recovered by affine translation of the OSM position within a certain maximum radius.

Let  $S_i$  be the OSM perimeter of a building (polygon), and  $T_{x,y}S_i$  be its translation by  $x$  meters horizontally (east-west) and  $y$  meters vertically (north-south). Let  $\hat{T}$  be the optimal translated position of the

Metric	$r_1 = 12m$		$r_2 = 8m$		$r_3 = 5.5m$	
	IoU	Distance	IoU	Distance	IoU	Distance
Average ( $\Delta_1 = 0.8m$ )	0.791	2.411	0.774	2.269	0.764	2.577
Median ( $\Delta_1 = 0.8m$ )	0.779	2.232	0.801	2.128	0.773	2.235
Average ( $\Delta_2 = 1.15m$ )	0.791	2.266	0.784	2.197	0.759	2.806
Median ( $\Delta_2 = 1.15m$ )	0.787	2.065	0.799	2.056	0.783	2.876

**Table 1:** Performance of the proposed position adjustment method for different values of  $r$ : IoU and distances between centroids of estimated locations and ground truth (higher values of IoU correspond to better fit).

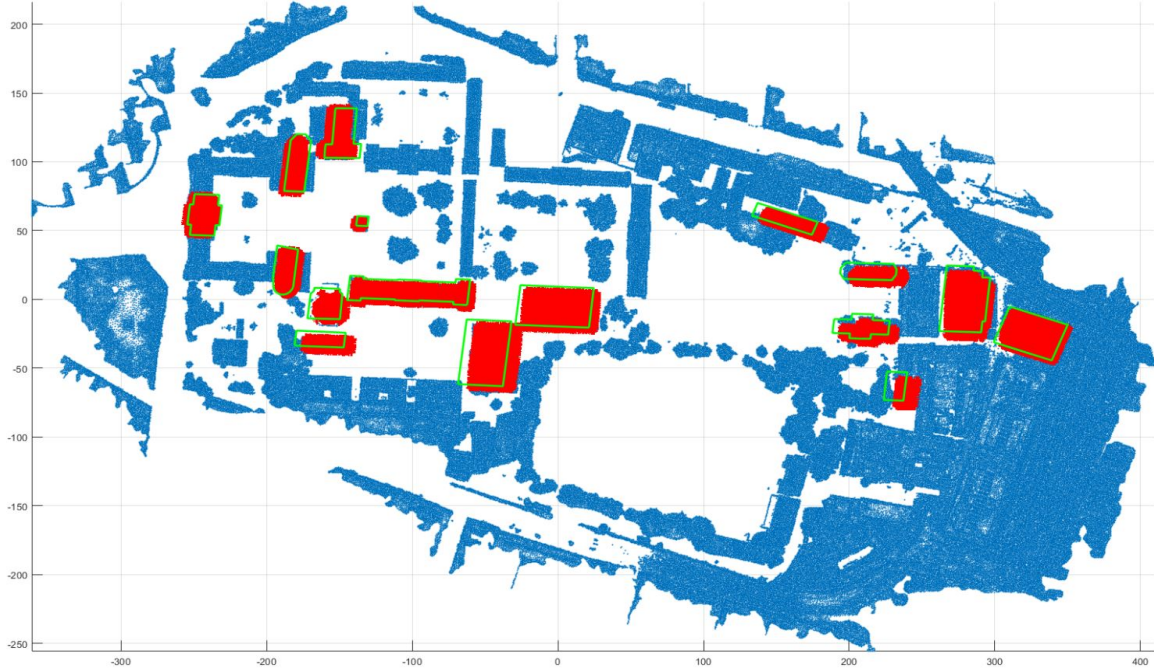


**Figure 6:** Fitting OSM to point cloud: blue patches are non-ground points from the point cloud (buildings and trees), green bounding boxes are original OSM structures, and in red are the estimated adjusted OSM positions.

OSM building delivering maximum to our fit criterion IoU, where we consider overlap between the OSM-translated polygon and the 2d point cloud. Then the perimeter of the building in our point cloud can be found as  $\hat{T}S_i$ , with

$$\hat{T} = \operatorname{argmax}_T \mathbf{IoU}(T_{x,y}S_i, D_{2d}), \text{ with } x^2 + y^2 < r^2.$$

To establish the overlap we also take into account the density of the 2d point cloud, which is non-uniform, due to substantially higher density of points along the edges of buildings (originating from points on the vertical surfaces).

Practically we simplify the above maximization problem by considering fixed sizes of increments for  $x$  and  $y$  translations in  $T_{x,y}$ . We apply two step sizes  $\Delta_1 = 1.15m$  and  $\Delta_2 = 0.8m$ , and conduct the search of the optimal position within the  $r_1 = 12m$ ,  $r_2 = 8m$  and  $r_3 = 5.5m$ . The overall result for  $(r_1, \Delta_1)$  is demonstrated in Fig. 6. The green polygon represents the initial OSM polygon, and the red data points are the segmented parts of the point cloud identified by our procedure.

In Fig. 5 we demonstrate the performance of adjustment procedure with the maximal radius increasing from  $r_3 = 5.5m$  to  $r_1 = 12m$  with a spatial translation step set to  $\Delta_1 = 1.15m$ . The initial OSM position for both highlighted buildings has a limited overlap with the point cloud data. For the Zoology building the IoU increases significantly from 0.15 (OSM after global registration) to 0.798 (after adjustment in  $r_3 = 12m$ ). Fig. 5a-5c demonstrates the gradual improvement of the OSM position with the increase of radius. In case of reasonably isolated buildings with little vegetation around this behaviour is typical. FitzGerald buildings in Fig. 5d-5f is an example of an isolated building closely surrounded by trees, which limits the performance of the position refinement procedure. Specifically, after the initial improvement from  $r_3 = 5.5m$  to  $r_2 = 8m$ , the estimated position in  $r_1 = 12m$  drops due to an adjacent cluster of dense tall vegetation which biases the estimated position.

Table 1 demonstrates performance of the proposed position adjustment algorithm for various values of search radius  $r$  and translation step  $\Delta$ . We show the average and median for these 16 buildings and we found that the IoU increases significantly. From 0.567 on average, after the global registration of OSM data, to above 0.75 after position adjustment. The distance between centroid point of polygons from 5.594 meters

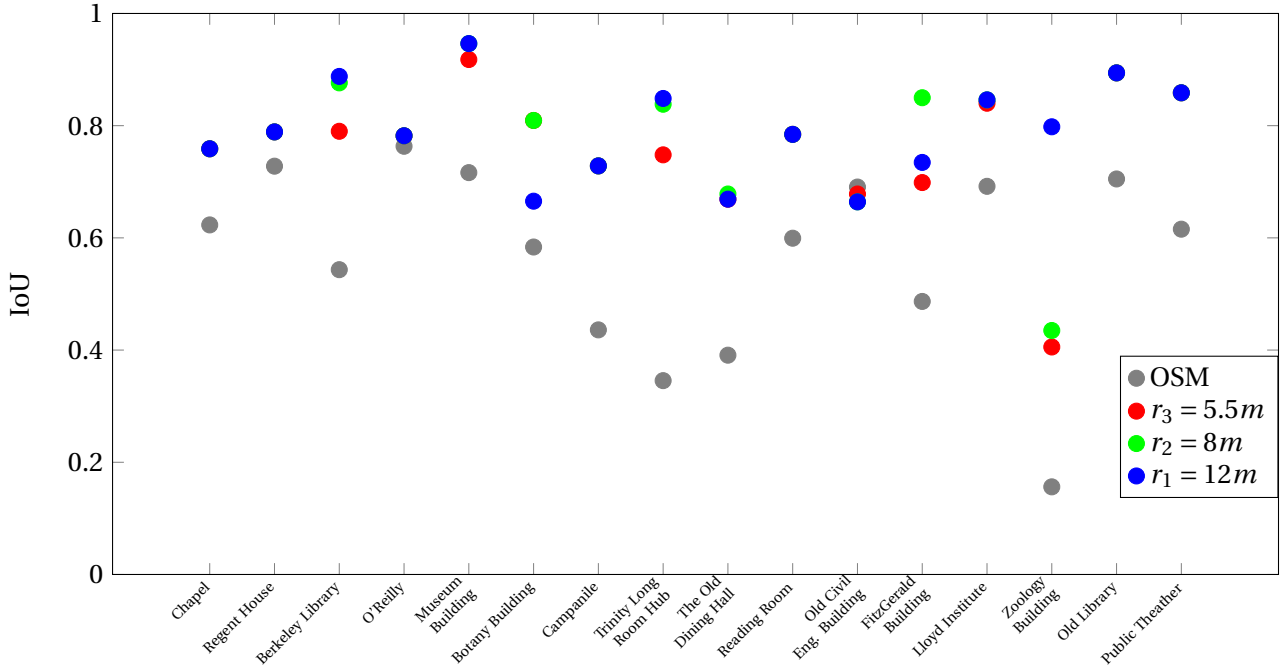


**Figure 7:** IoU per building: initial OSM (after global affine registration) and adjusted position with three radii  $r$ .

down to around 2-2.4 meters after automatically estimated translation adjustment  $\hat{T}$ . In addition, in Fig. 7 we demonstrate the improvement in IoU achieved with the proposed position adjustment approach for the considered individual buildings with the translation step  $\Delta_2 = 1.15m$  and three radii  $r$ . The proposed greedy search strategy consistently improves the overlap between OSM shapes and point cloud data. We implement this algorithm on CPU(Intel i7 with 8 threads) in MATLAB. The whole segmentation process takes around 6-8 minutes depending on maximum distance  $r_i$  and step  $\Delta_i$ .

## 5 Conclusion & Future work

Our overall results show that aligning GIS (OSM) data with 3D point cloud is promising for segmenting it in meaningful subsets of vertices. We are currently working on improving the robustness of the pipeline by integrating the colour information into the decision process.

## Acknowledgement

This work was supported by the ADAPT Centre for Digital Content Technology, funded by the Science Foundation Ireland Research Centres Programme (Grant 13/RC/2106) and the European Regional Development Fund.

## References

- [Agarwal et al., 2009] Agarwal, S., Snavely, N., Simon, I., Sietz, S. M., and Szeliski, R. (2009). Building rome in a day. In *Twelfth IEEE International Conference on Computer Vision (ICCV 2009)*, Kyoto, Japan. IEEE.
- [Becker et al., 2017] Becker, C., Häni, N., Rosinskaya, E., d'Angelo, E., and Strecha, C. (2017). Classification of aerial photogrammetric 3d point clouds. *ISPRS Annals of Photogrammetry, Remote Sensing and Spatial Information Sciences*, IV-1/W1:3–10.

- [Bódis-Szomorú et al., 2016] Bódis-Szomorú, A., Riemenschneider, H., and Gool, L. V. (2016). Efficient volumetric fusion of airborne and street-side data for urban reconstruction. In *2016 23rd International Conference on Pattern Recognition (ICPR)*, pages 3204–3209.
- [Branson et al., 2018] Branson, S., Wegner, J. D., Hall, D., Lang, N., Schindler, K., and Perona, P. (2018). From google maps to a fine-grained catalog of street trees. *ISPRS Journal of Photogrammetry and Remote Sensing*, 135:13 – 30.
- [Bulbul and Dahyot, 2017] Bulbul, A. and Dahyot, R. (2017). Social media based 3d visual popularity. *Computers & Graphics*, 63:28 – 36.
- [Byrne et al., 2017] Byrne, J., Connelly, J., Su, J., Krylov, V., Bourke, M., Moloney, D., and Dahyot, R. (2017). Trinity college dublin drone survey dataset. Technical report, School of Computer Science & Statistics, Trinity College Dublin.
- [Byrne et al., 2017] Byrne, J., Laefer, D. F., and O’Keeffe, E. (2017). Maximizing feature detection in aerial unmanned aerial vehicle datasets. *Journal of Applied Remote Sensing*, 11(2):025015.
- [Csurka et al., 2013] Csurka, G., Larlus, D., Perronnin, F., and Meylan, F. (2013). What is a good evaluation measure for semantic segmentation? In *BMVC*, volume 27.
- [Haahr, 2017] Haahr, M. (2017). Creating location-based augmented-reality games for cultural heritage. In Alcañiz, M., Göbel, S., Ma, M., Fradinho Oliveira, M., Baalsrud Hauge, J., and Marsh, T., editors, *Serious Games*, pages 313–318, Cham. Springer International Publishing.
- [Kaiser et al., 2017] Kaiser, P., Wegner, J. D., Lucchi, A., Jaggi, M., Hofmann, T., and Schindler, K. (2017). Learning aerial image segmentation from online maps. *IEEE Transactions on Geoscience and Remote Sensing*, 55:6054–6068.
- [Krylov and Dahyot, 2018] Krylov, V. and Dahyot, R. (2018). Object geolocation using mrf-based multi-sensor fusion. In *Proc. of IEEE Int’l Conf on Image Processing ICIP*, Athens, Greece.
- [Krylov et al., 2018] Krylov, V. A., Kenny, E., and Dahyot, R. (2018). Automatic discovery and geotagging of objects from street view imagery. *Remote Sensing*, 10(5).
- [Laefer et al., 2017] Laefer, D. F., Abuwarda, S., Vo, A.-V., Truong-Hong, L., and Gharibi, H. (2017). 2015 aerial laser and photogrammetry survey of dublin city collection record. Technical report, New York University. 3D point cloud dataset. <https://doi.org/10.17609/N8MQ0N>.
- [Riemenschneider et al., 2014] Riemenschneider, H., Bódis-Szomorú, A., Weissenberg, J., and Van Gool, L. (2014). Learning where to classify in multi-view semantic segmentation. In Fleet, D., Pajdla, T., Schiele, B., and Tuytelaars, T., editors, *Computer Vision – ECCV 2014*, pages 516–532. Springer.
- [Rumpler et al., 2012] Rumpler, M., Irschara, A., Wendel, A., and Bischof, H. (2012). *Rapid 3D City Model Approximation from Publicly Available Geographic Data Sources and Georeferenced Aerial Images*, pages 1–8. .
- [Tchapmi et al., 2017] Tchapmi, L. P., Choy, C. B., Armeni, I., Gwak, J., and Savarese, S. (2017). Segcloud: Semantic segmentation of 3d point clouds. In *International Conference on 3D Vision (3DV)*.
- [Tighe and Lazebnik, 2010] Tighe, J. and Lazebnik, S. (2010). SuperParsing: Scalable Nonparametric Image Parsing with Superpixels. In Daniilidis, K., Maragos, P., and Paragios, N., editors, *Computer Vision – ECCV 2010*, pages 352–365, Berlin, Heidelberg. Springer Berlin Heidelberg.